

Combining Dyad Protonation and Active Site Plasticity in BACE-1 Structure-Based Drug Design

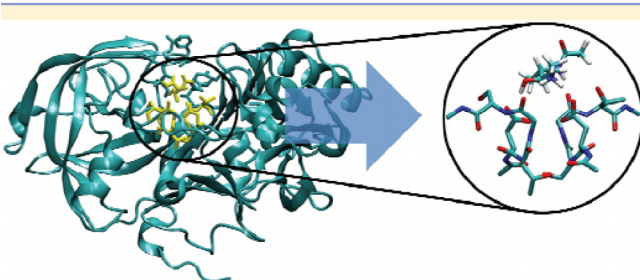
Puneet Kacker,[†] Matteo Masetti,[‡] Martina Mangold,[§] Giovanni Bottegoni,^{*,†} and Andrea Cavalli^{*,‡,†}

[†]Department of Drug Discovery and Development, Istituto Italiano di Tecnologia, via Morego 30, 16163 Genova, Italy

[‡]Department of Pharmaceutical Sciences, Alma Mater Studiorum – Università di Bologna, Via Belmeloro 6, 40126 Bologna, Italy

[§]Department of Chemistry, Cambridge University Centre of Computational Chemistry, Lensfield Road, CB2 1EW Cambridge, United Kingdom

Supporting Information



ABSTRACT: The ability of the BACE-1 catalytic dyad to adopt multiple protonation states and the conformational flexibility of the active site have hampered the reliability of computational screening campaigns carried out on this drug target for Alzheimer's disease. Here, we propose a protocol that, for the first time, combining quantum mechanical calculations, molecular dynamics, and conformational ensemble virtual ligand screening addresses these issues simultaneously. The encouraging results prefigure this approach as a valuable tool for future drug discovery campaigns.

Alzheimer's disease (AD) is a neurodegenerative disorder and a major cause of dementia among elderly people. At neuronal level, AD is characterized by amyloid- β ($A\beta$) plaques, which are predominantly aggregates of $A\beta$ peptide, a small 40–42 amino acids long peptide generated by the proteolytic cleavage of the transmembrane Amyloid Precursor Protein (APP),¹ operated by two proteases, β - and γ -secretase. Recent clinical trials have shown that while a γ -secretase inhibitor failed in phase III clinical trials,² a β -secretase inhibitor is still actively investigated in phase II.³ This makes β -secretase one of the few valuable targets for testing the amyloid hypothesis in AD.⁴ The β -secretase protease (β -site APP cleaving enzyme, BACE-1, EC 3.4.23.46) belongs to the aspartic proteases family, and as such, its catalytic machinery encompasses two Aspartic acid residues (Asp32 and Asp228, simply referred to as the dyad). The enzymatic reaction takes place according to the rules of general acid–base catalysis with a water molecule acting as nucleophile.⁵ In presence of the substrate, the overall charge on the dyad is -1 : one of the dyad members is protonated, whereas the other is negatively charged. Experimental evidence has shown that different functional groups present on

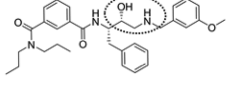
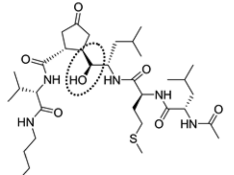
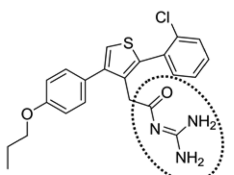
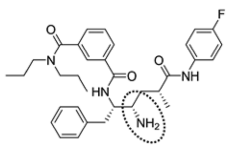
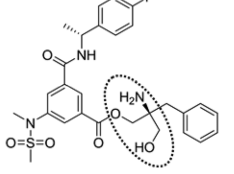
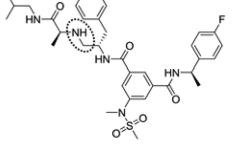
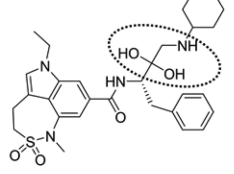
chemically diverse BACE-1 inhibitors can stabilize the dyad in different protonation states. This can alter the dyad overall charge and modify the exact location of the proton.⁶ Several authors attempted to identify the most probable dyad protonation state with molecular and quantum mechanics (QM) studies. Park and Lee⁷ performed molecular dynamics (MD) simulations on BACE-1 in complex with the peptidomimetic inhibitor OM99–2 (PDBid: 1FKN).⁸ In their study, only two different protonation models were considered. The strength of the H-bond interactions between ligand and protein was monitored throughout the trajectories and used as a criterion to assign the most favorable protonation state. Rajamani and Reynolds⁹ modeled eight possible dyad protonation states using a linear-scaling quantum mechanical program on the basis of a divide and conquer approach (DIVCON). Their semi-empirical quantum mechanical method was used to identify the most probable protonation state of the enzyme in the apo form and when in complex with OM99–2. Recently, the effects of the dyad protonation on inhibitor affinity¹⁰ and virtual ligand screening (VLS)¹¹ have also been discussed. In their seminal work, Polgár and Keserü have compared the effect of different protonation states on VLS studies employing different docking engines and scoring functions. Besides protonation state variability, BACE-1 binding pocket displays also remarkable conformational flexibility, mainly due to the high plasticity of the so-called flap region (residues 68–74) and the 10s loop (residues 9–14).¹¹ Crystallographic evidence confirm that these regions are selectively stabilized in different conformations by different inhibitors, hence the importance of considering multiple pocket rearrangements in structure-based hit discovery. Multiple receptor conformations (MRC) VLS was indeed adopted by several groups as a straightforward method to take into account receptor flexibility, and it contributed to identify novel hits in BACE-1 inhibitors drug discovery campaigns.^{12–14} For a comprehensive review on the most important milestones in BACE-1 computational drug discovery, the interested reader is addressed to the exhaustive report of McGaughey and Holloway.¹⁵

Most of the studies reported so far focused only on one structure, namely that of the complex formed between BACE-1 and OM99–2, and despite the ever increasing number of crystallographic structures deposited, a systematic computational

Published: February 8, 2012



Table 1. Representative Chemical Structures of BACE-1 Inhibitors

Cluster	Interacting group	#complexes	Representative	Structure ¹	DFT-assigned protonation states	DFT+MD-assigned protonation states
1	Hydroxyethylamine	30	1W51		32i, 228o	32i
2	Hydroxyethylene	5	1YM2		32i, 228o	32i
3	Acylguanidine	4	2QU3		228i, ddp	228i, ddp
4	Primary Amine	5	2FDP		228i	228i
5	Hydroxy and Primary amine	1	2IS0		32o, 228i	228i
6	Reduced Amide	1	2QZL		32i, 32o, 228i	32i, 228i
7	Di-hydroxyethylamine	1	2WF4		32i, 228i	32i, 228i

¹Each ligand interacting group is highlighted by a dotted ellipse.

study on the effect of different ligands on the dyad protonation state has never been attempted. Moreover, the issues related to dyad protonation and binding site conformational plasticity have always been addressed separately, leading to a simplified and partial description of a very complex system. Here, using multiple BACE-1 inhibitors cocrystals, we report on a study that, for the first time, aims at characterizing the role concurrently played by dyad protonation along with binding pocket plasticity upon inhibitor binding in VLS campaigns.

A methodical investigation of 146 enzyme–inhibitor complexes available in the PDB (as of January 2011) led to the identification of 47 high quality BACE-1 crystal structures (see also Supporting Information, SI). These structures were parted into seven clusters based on the functional groups of the

inhibitors interacting with the dyad (see Table 1). Ligands displaying a hydroxyethylamine (HEA) interacting group formed the most populated cluster (30 complexes). HEA is a noncleavable transition state isostere that has been extensively employed in the development of BACE-1 and other aspartic protease inhibitors.^{16,17} The results of the calculations carried out on this highly populated cluster will be reported and discussed extensively as a case study. Details on QM calculations, MD simulations, and docking results for all the other clusters are reported in the SI.

A systematic QM characterization on a representative structure from each cluster was performed in the Density Functional Theory (DFT) framework. The goal was to identify the most energetically favorable dyad protonation state in

presence of a certain interacting group.¹⁵ Five discrete protonation states were therefore considered for each representative structure: the four possible monoprotonated states (hereafter labeled as 32i, 32o, 228i, and 228o, where the digit stands for the residue number, while the letter indicates whether the proton is carried by the inner or the outer oxygen atom) and the dideprotonated state (labeled as ddp). In order to compare energies between protonation states carrying a different net charge, a suitable isodesmic reaction was exploited (see SI, Methods). Although a more rigorous approach based on the estimation of free energy differences can be conceived,¹⁸ to take properly into account both solvation effects and conformational flexibility, an additional computational demand would be required. For sake of the efficiency of the protocol, we therefore preferred to employ a more naïve approach based on a simple and straightforwardly achievable estimation of electronic energies. The results reported in Table 1 confirmed that the dyad preferentially adopted different states according to the chemical nature of the binder. In several cases, the protonation state with the best energy profile was only marginally more stable than one of the others (less than 2.0 kcal/mol) (see SI, Table S3).

For this reason, results were evaluated not only in terms of energetic stability but also of deviation with respect to the crystallographic structure. In fact, it has been recently reported that the carboxyl groups' coplanarity level is a structural feature that plays an important role in the binding event and can be used as an additional marker of stability.¹⁹ Moreover, to assess the reliability of the protocol, all the QM results displaying energy differences less than 2.0 kcal/mol were further investigated by means of MD simulations (see SI). In this way, it was possible to discard the protonation states in which a tight H-bond network and a stable binding of the substrate could not be maintained along the trajectories. In four out of six cases in which DFT calculations could not unambiguously pinpoint a single most stable protomer, the analysis of the trajectories allowed us to narrow the number of possible candidates further down. The results of this sequential selection procedure that combines QM calculations and MD simulations are reported in Table 1. In the cases of clusters 3, 6, and 7, when two protomers both displayed good electronic energy and substantial stability along the MD trajectories, they were considered equally probable and assigned together. Collectively, our results pointed toward a generalized preference for inner protonation states, in agreement with previously reported data.

The QM calculations performed on the representative structure of the HEA interacting group cluster (PDBid: 1W51) assigned the most favorable energy to 228o. However, in 228o, the crystallographic geometry of the dyad was lost after QM optimization (rmsd 0.67 Å), with the distance between inner O³² and inner O²²⁸ (hereafter simply referred to as inner O³² – inner O²²⁸ distance) increasing up to 3.30 Å. The relative energy of 32i was very close to 228o ($\Delta E < 0.2$ kcal/mol), and the dyad maintained the crystal conformation after DFT optimization. As illustrated in Figure 1, the HEA charged amine nitrogen formed H-bond and electrostatic interactions with the outer carboxyl oxygen of Asp228 and the backbone carbonyl of Gly34. The hydroxyl group of the ligand donated an H-bond to the outer oxygen of Asp32. We also examined the different stability between the inner states. The main difference was that while in 32i, the hydroxyl group of Thr231 established a strong H-bond interaction with the outer carboxyl oxygen of Asp228, in 228i, this interaction was much weaker, as reflected by an energy

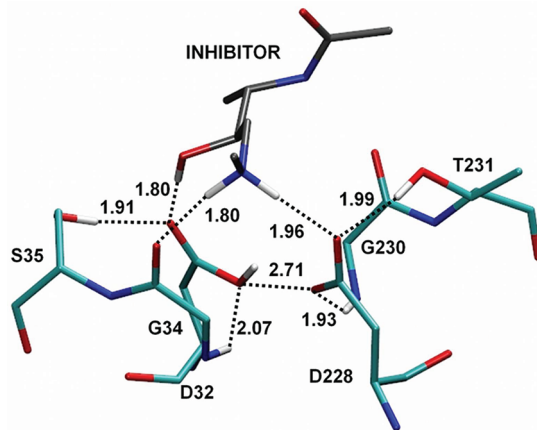


Figure 1. B3LYP optimized geometry of 1W51 binding pocket. For clarity, only important residues are reported. Key H-bonds are highlighted by dotted black lines; their lengths in angstroms are explicitly reported. Inhibitor carbon atoms are shown in gray.

difference of 2.0 kcal/mol. MD simulations were performed to further investigate the relative stability of states 32i and 228o and, hence, to assess the reliability of QM results, which were driven by combining energetic and geometric considerations. Over the 2 nanoseconds of simulation, the complexes in the considered protonations states showed a fairly good overall structural stability, as evidenced by the rmsd calculated either on the C α atoms or on the heavy atom of the ligand, which was approaching about 1.5 Å in both cases (see Figure 2a and b, respectively). To better discern structural deviations in proximity of the dyad, two local geometrical descriptors were employed: the inner O³² – inner O²²⁸ distance and the dihedral angle formed by the four oxygens of the dyad (OD1³²-OD2³²-OD1²²⁸-OD2²²⁸). As it can be inferred by Figure 2c and d, the 32i state showed a greater stability compared to 228o, confirming the QM results. In particular, during the MD simulation, the 228o state converted to 228i by a χ_2 flipping occurring at about 700 ps (see Figure 2d). In conclusion, MD simulations supported the 32i as most stable state in line with QM calculations.

We then investigated how the protonation states could affect the outcome of hit generation endeavors. Self-docking simulations were performed on each structure considering independently the aforementioned protonation states. Using conformations that are perfectly adapted to the inhibitor, this self-docking exercise allowed us to assess the pure contribution of the dyad protonation to the formation of the docked complex. A near-native pose (within 2.0 Å rmsd from the crystallographic position of the ligand non-hydrogen atoms) was obtained in 85.1% of the cases (40 complexes) when the protonation state indicated by DFT calculations was used. In 61.7% (29 complexes), it was also possible to reproduce the specific H-bond interactions between the interacting group and dyad. Furthermore, in 25 of these 29 cases, the complex with the DFT predicted protonation state provided also the best binding score. In the HEA cluster, all protonation states performed very accurately (see Figure 3a). In 90.0% of the complexes, a near-native pose could always be ranked within the top five scoring conformations regardless of the assigned protonation state (see Figure 3b), and each crystallographic complex could always be reproduced in at least one protonation state (100.0% combined success rate). Mainly because of the rmsd-based success criterion, the average size (584.1 MW) and

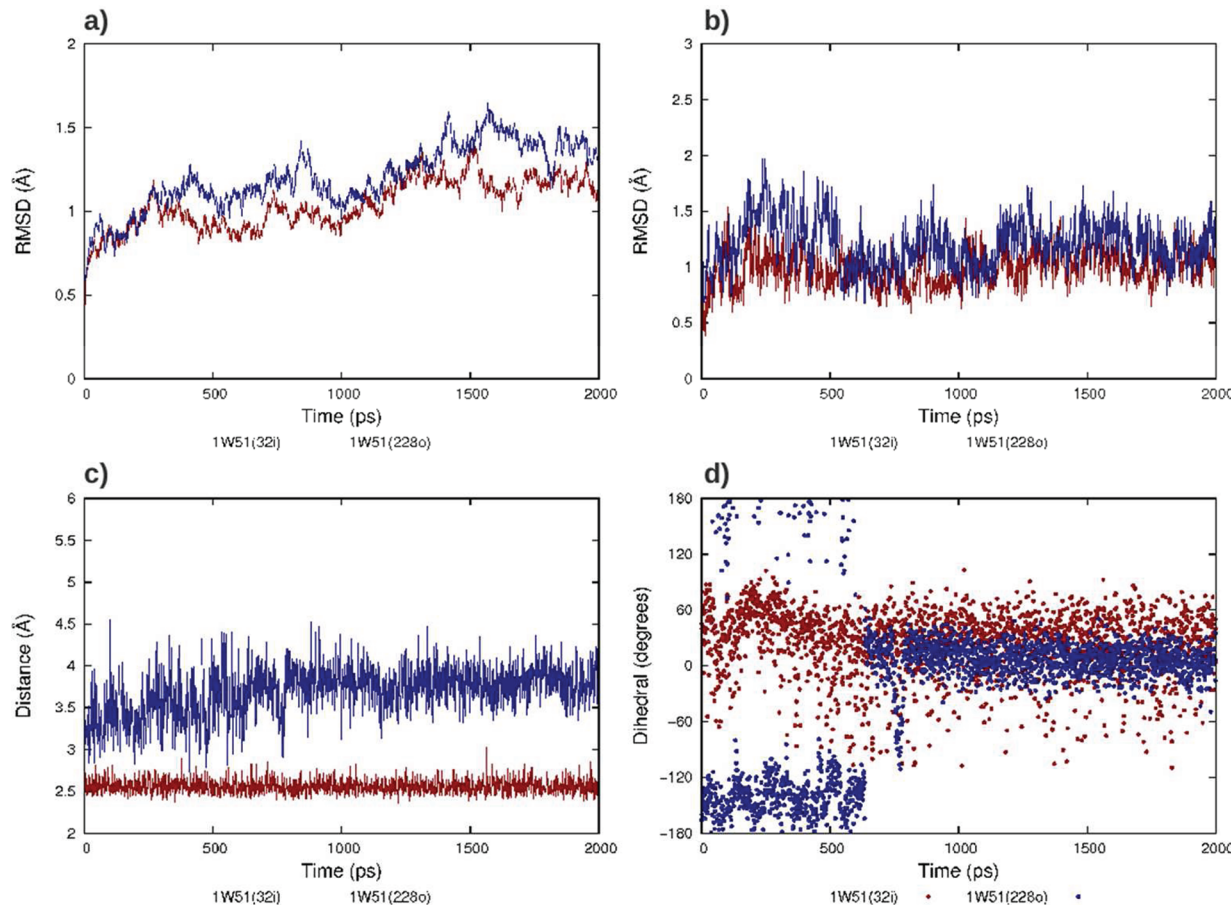


Figure 2. Analysis of the MD trajectory for the representative structure of cluster 1 (1W51) in the two considered protonation states: 32i (red lines and dots) and 228o (blue lines and dots). (a) rmsd calculated on the C_α atoms, (b) rmsd calculated on the heavy atoms of the ligand, (c) inner O³² – inner O²²⁸ distance, and (d) dihedral angle formed by the four oxygens of the dyad.

volume (588.9 Å³) of HEA interacting group inhibitors belittled the relevance of the dyad protonation state on docking accuracy. rmsd is a measure universally adopted because it is very intuitive and easy to calculate. However, it here appeared particularly ill fitted, lacking the ability to provide any insights on specific interactions at the molecular level.²⁰ However, when the ability of the interacting group to establish two direct H-bond interactions with the dyad (one between the hydroxyl group of the ligand and the outer oxygen of Asp32, the other between the charged amine nitrogen and the outer carboxyl oxygen of Asp228) was added as a second requirement to fulfill, the only states to retain a significant success rate (56.0%) were 32i and ddp (see Figure 3c). Interestingly, 32i complexes scored systematically better than those obtained with ddp, in good agreement with DFT-based predictions.

After highlighting the key role of dyad titration in ligand binding by means of self-docking, more challenging cross-docking simulations were carried out to investigate the role of receptor flexibility. Cross-docking studies were performed on nonsingleton clusters (i.e., clusters 1–4). Within each cluster, ligands were independently docked at each receptor conformation, and each receptor conformation was represented in all five protonation states. Cross-docking was considered successful when (i) a near-native structure was ranked within the top 10 poses and (ii) the interacting group could establish direct interactions with the dyad. In cluster 1, when the receptor was assigned the protonation state predicted by DFT

and MD studies, namely 32i, the results' accuracy significantly improved. In cluster 2, the best results were obtained with 228o, which was assigned a favorable energy by DFT calculations but lacked stability in MD simulations. In the other two cases, while 228i, the state predicted by DFT and MD calculations to provide the tightest interaction with the interacting group, led nonetheless to good results, the state providing the best docking scores turned out to be ddp. These two clusters display charged interacting groups, namely acylguanidine and primary amine, so these results can be explained by the well-known tendency of scoring functions to overestimate Coulombic interactions.²¹ According to these results, not only self-docking but also cross-docking success rate steeply depends on dyad titration. In cross-docking studies performed on the HEA cluster, 30 ligands and 150 receptor variants (30 receptor conformations by 5 protonation states) were considered. Success rates for individual runs ranged from 36.7% (11 ligands in PDBid: 1W51, 32o) to 90.0% (27 ligands in PDBid: 2WEZ, 32o), with a median value of 73.3% (22 ligands correctly reproduced). Remarkably, it was always possible to reproduce the native pose of each ligand in at least one receptor variant. No ligand behaved as a universal binder, namely displaying the native pose in all pocket rearrangements. In terms of energy, 46.9% of the ligands achieved their overall best score using 32i protonation state, a fraction significantly higher than any of the other four (see Figure 3d), and in good agreement with DFT, MD, and self-docking outcomes.

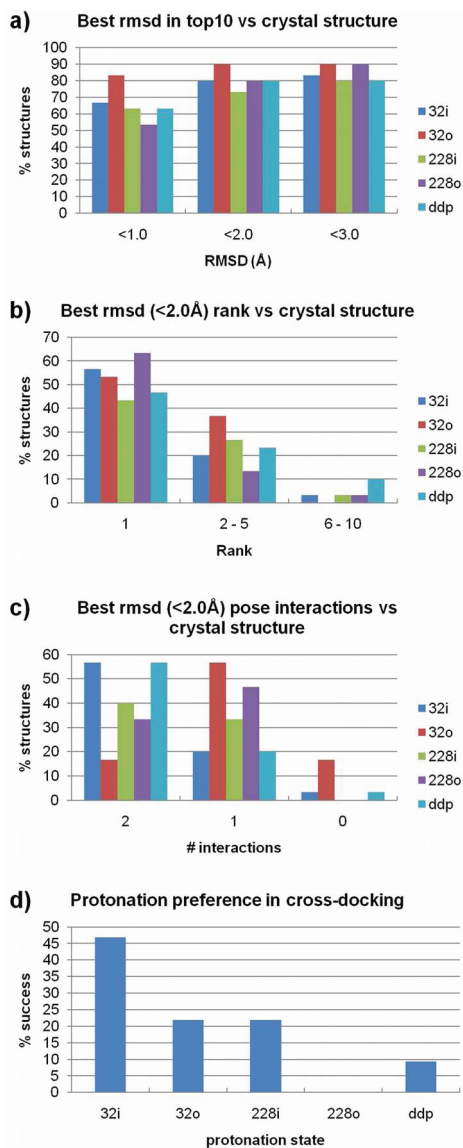


Figure 3. Results of docking studies. (a) Distribution of rmsd values between the closest among the top 10 ranking poses (lowest deviation) and the corresponding crystal structure for each complex in self-docking studies. (b) Rank distribution of the best ranking near-native pose in self-docking studies. (c) Distribution of near-native poses as a function of dyad-interacting group number of interactions in self-docking studies. (d) Cross-docking success rate.

No ligand obtained the best score using the 228o variant, suggesting that this protonation state is the less likely to generate optimal interactions with HEA. Cross-docking success rates for each receptor variant are reported in Figure 4.

To apply the insights gained so far to a hit discovery exercise, two sets of BACE-1 conformations were compiled and tested in an advanced VLS protocol. In the first set (DFT-MD set), at least one structure from each cluster was selected, and the most favorable protonation states as predicted by the combined application of DFT calculations and MD simulations were assigned. To account for intracluster pocket flexibility, multiple members from clusters 1 and 4 were included. Eventually, the first collection encompassed a combination of 13 different conformers and protomers that captured the variability of the binding pocket flexible regions. In the second set (DOCK set), the same conformers were selected, but protonation states were assigned according to the best success rates identified in retrospective docking studies. The second ensemble encompassed 10 receptor variants.

A matrix of relevant rms distances among binding site residues in different conformers is reported in Figure S11 of SI.

The ability of these ensembles to separate binders from nonbinders in VLS studies enriching active molecules in the topmost ranking fraction was assessed by means of two ligand data sets. In the first test screening, a data set previously compiled by Craig and colleagues,¹³ which originally comprised 59 binders and 408 bona fide nonbinders, was used. In Table 2, VLS results are reported adopting the Boltzmann-Enhanced Discrimination of Receiver Operating Characteristics metric (BEDROC) as a figure of merit. BEDROC assesses the overall performance of the protocol, assigning a privileged weight to binders enriched in the top-ranking fraction.²² The individual performance of each conformer was rather poor. The benchmark included heterogeneous BACE-1 inhibitors, while each receptor variant was here selected because of its ability to complement only ligands displaying one specific interacting group. However, when the results from independent runs were combined, the accuracy of the MRC protocol outperformed every single conformer (DFT-MD Combined BEDROC 0.73; DOCK Combined BEDROCK 0.78; see Table 2). In individual runs of the DFT-MD set variants. True binders enriched in the topmost 10% were on average 22, never exceeding 28, while in the combined ranking, 31 binders could be selected. In the DOCK set, true binders enriched in the topmost 10% were on average 24, never exceeding 29. In this case, in the combined ranking, 35 binders were enriched in the topmost 10%. Comparing the performances of the two sets, it is possible to note that the DFT-MD set could efficiently separate binders from nonbinders without relying on insights gained through retrospective self- and cross-docking studies. However, if this kind of information were indeed available, it could be efficiently plugged into the MRC screening protocol to further improve its performance, as suggested by the DOCK set combined BEDROC. Moreover, binders mostly obtained their best score in runs employing the receptor variant cocrystallized with a

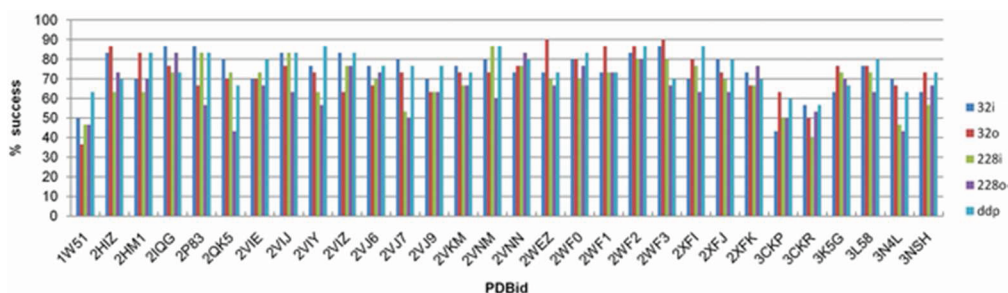


Figure 4. Distribution of cross-docking success rate as a function of receptor conformation.

Table 2. BEDROC Metrics Calculated for Each BACE-1 Structure

Cluster	PDBid	DFT-MD-based selection			Docking-based selection		
		Protonation state	Craig data set	HEA decoys	Protonation state	Craig data set	HEA decoys
1	2IQG	32i	0.67	0.91	32i	0.67	0.91
1	2P83	32i	0.63	0.83	32i	0.63	0.83
1	2WF3	32i	0.62	0.92	32i	0.62	0.92
2	1YM2	32i	0.44	0.65	228o	0.47	0.47
3	2ZDZ	228i	0.17	0.12	ddp	0.19	0.20
		ddp	0.19	0.20			
4	2FDP	228i	0.52	0.86	ddp	0.68	0.75
4	2IRZ	228i	0.59	0.51	ddp	0.68	0.59
5	2ISO	228i	0.62	0.59	228i	0.62	0.59
6	2QZL	32i	0.57	0.83	32i	0.57	0.83
		228i	0.56	0.58			
		combined	0.73	0.85	combined	0.78	0.87
7	2WF4	228i	0.54	0.96	228i	0.54	0.96
		32i	0.58	0.97			

ligand displaying the same or a very close interacting group (see SI, Figure S12). These results showed that the proposed set of receptor variants could not only increase the number of active molecules enriched in the top-ranking fraction but prioritizing molecules with different interacting groups could also enhance their chemical diversity.²³ To further prove this point, we measured the separating power of the sets if all receptor variants were naïvely assigned a ddp protonation state. The combined BEDROC turned out to be 0.76; a result that is only apparently in line with the previous ones. In fact, in the naïve ddp case, the BEDROC score is determined by the efficient enrichment of a limited number of chemotypes. For example, ligands displaying the hydroxyethylene IG disappeared altogether from the topmost ranking fraction.

To test whether the proposed MRC approach could handle binders' enrichment within a specific class of molecules, a second test set was assembled collecting binders only from cluster 1 cocrystallized ligands (30 ligands) and purposely selecting 118 very challenging decoys (structures included in the SI). Decoys explicitly carried a HEA moiety and matched the atomic property fields' signature of the binders.²⁴ VLS performance on this set is reported in Table 2. As expected, receptor structures from cluster 1 provided good enrichments with BEDROC values of 0.91, 0.83, and 0.92, respectively. A very good performance was also obtained employing the receptor structure from cluster 7 (PDBid: 2WF4), which is characterized by an interacting group very similar to that of cluster 1 (dihydroxyethylamine) and was assigned a compatible protonation state (32i/228i in DFT-MD and 228i in DOCK). Inversely, structures displaying different pocket rearrangements and protonation states achieved significantly worse performances. In DFT-MD set, combining individual results, it was possible to obtain a BEDROC value of 0.85, outperforming 8 conformers out of 13 and in line with the results generated by adapted structures from cluster 1. In the DOCK set, the combined BEDROC value was 0.87, outperforming 7 conformers out of 10. To put these figures in the right perspective, it is worth to emphasize that, in a nonretrospective study, it is very hard to predict *a priori* which conformer will provide the best results.²⁵ In line with the expectations, this time the difference between the performances of the two sets of receptor variants was minimal, considering that in both sets conformers from cluster 1 were assigned the same protonation state. Overall, results on the second ligand benchmark showed that

the proposed MRC approach, despite being geared to promote chemical diversity, could efficiently enrich a specific chemical class managing the noise introduced by nonadapted conformers and protomers. The results are in line with those obtained assigning to all conformers in the set the ddp protonation state, particularly suitable because of the charged nature of the HEA IG (combined BEDROC 0.91) or the ideal 32i (combined BEDROC 0.95).

In summary, we systematically studied the combined effect that dyad protonation and binding pocket conformation have on docking and VLS simulations carried out on BACE-1. Previously reported VLS schemes lacked the ability to tackle these two issues at the same time, and possibly for this reason, computer-assisted methods have had limited impact upon the development of new BACE-1 inhibitors. In fact, it has turned out that so far a combination of *in vitro* screening and structure-guided SAR development has been the most successful strategy in obtaining low nanomolar inhibitors for this target.¹⁶ Plugging evidence gathered through QM calculations and MD simulations in our well-established MRC screening approach,²⁵ we devised a practical tool for those involved in the study of BACE-1. The reported protocol was tested for its ability to separate binders from nonbinders in challenging conditions, and yet the results turned out to be particularly good in terms of overall score and specific interactions established with the dyad. For these reasons, we believe that the insights gained from our study will improve the relevance of computational methods in BACE-1 inhibitors discovery campaigns.

ASSOCIATED CONTENT

S Supporting Information

All computational methods and details on data collection. Clusters 2–7 QM, MD, docking, and VLS detailed results. This material is available free of charge via the Internet at <http://pubs.acs.org>.

AUTHOR INFORMATION

Corresponding Author

*E-mail: giovanni.bottegoni@iit.it; andrea.cavalli@iit.it.

Notes

The authors declare no competing financial interest.

ACKNOWLEDGMENTS

The authors thank Walter Rocchia for the helpful discussions on VLS performance assessment and the IIT Platform "Computation".

REFERENCES

- (1) Citron, M. Alzheimer's disease: Strategies for disease modification. *Nat. Rev. Drug Discov.* **2010**, *9*, 387–398.
- (2) Kelleher, R. J., III; Shen, J. γ -Secretase and human disease. *Science* **2010**, *330*, 1055–1056.
- (3) Klaver, D. W.; Wilce, M. C.; Cui, H.; Hung, A. C.; Gasperini, R.; Foa, L.; Small, D. H. Is BACE1 a suitable therapeutic target for the treatment of Alzheimer's disease? Current strategies and future directions. *Biol. Chem.* **2010**, *391*, 849–859.
- (4) Huang, W. H.; Sheng, R.; Hu, Y. Z. Progress in the development of nonpeptidomimetic BACE 1 inhibitors for Alzheimer's disease. *Curr. Med. Chem.* **2009**, *16*, 1806–1820.
- (5) Turk, B. Targeting proteases: Successes, failures and future prospects. *Nat. Rev. Drug Discov.* **2006**, *5*, 785–799.
- (6) Domínguez, J. L.; Christopeit, T.; Villaverde, M. C.; Gossas, T.; Otero, J. M.; Nyström, S.; Baraznenok, V.; Lindstrom, E.; Danielson, U. H.; Sussman, F. Effect of the protonation state of the titratable residues on the inhibitor affinity to BACE-1. *Biochemistry* **2010**, *49*, 7255–7263.
- (7) Park, H.; Lee, S. Determination of the active site protonation state of β -secretase from molecular dynamics simulation and docking experiment: implications for structure-based inhibitor design. *J. Am. Chem. Soc.* **2003**, *125*, 16416–16422.
- (8) Hong, L.; Koelsch, G.; Lin, X.; Wu, S.; Terzyan, S.; Ghosh, A. K.; Zhang, X. C.; Tang, J. Structure of the protease domain of memapsin 2 (β -secretase) complexed with inhibitor. *Science* **2000**, *290*, 150–153.
- (9) Rajamani, R.; Reynolds, C. H. Modeling the protonation states of the catalytic aspartates in β -secretase. *J. Med. Chem.* **2004**, *47*, 5159–5166.
- (10) Polgár, T.; Keserü, G. M. Virtual screening for β -secretase (BACE1) inhibitors reveals the importance of protonation states at Asp32 and Asp228. *J. Med. Chem.* **2005**, *48*, 3749–3755.
- (11) Gorfe, A. A.; Caflisch, A. Functional plasticity in the substrate binding site of β -secretase. *Structure* **2005**, *13*, 1487–1498.
- (12) Limongelli, V.; Marinelli, L.; Cosconati, S.; Braun, H. A.; Schmidt, B.; Novellino, E. Ensemble-docking approach on BACE-1: Pharmacophore perception and guidelines for drug design. *Chem-MedChem* **2007**, *2*, 667–678.
- (13) Craig, I. R.; Essex, J. W.; Spiegel, K. Ensemble docking into multiple crystallographically derived protein structures: an evaluation based on the statistical analysis of enrichments. *J. Chem. Inf. Model.* **2010**, *50*, 511–524.
- (14) Polgár, T.; Keserü, G. M. Ensemble docking into flexible active sites. Critical evaluation of FlexE against JNK-3 and β -secretase. *J. Chem. Inf. Model.* **2006**, *46*, 1795–1805.
- (15) McGaughey, G. B.; Holloway, M. K. Structure-guided design of β -secretase (BACE-1) inhibitors. *Expert Opin. Drug Dis.* **2007**, *2*, 1129–1138.
- (16) Silvestri, R. Boom in the development of non-peptidic β -secretase (BACE1) inhibitors for the treatment of Alzheimer's disease. *Med. Res. Rev.* **2009**, *29*, 295–338.
- (17) Bursavich, M. G.; Rich, D. H. Designing non-peptide peptidomimetics in the 21st century: Inhibitors targeting conformational ensembles. *J. Med. Chem.* **2002**, *45*, 541–558.
- (18) Yu, N.; Hayik, S. A.; Wang, B.; Liao, N.; Reynolds, C. H.; Merz, K. M. Assigning the protonation states of the key aspartates in β -secretase using QM/MM X-ray structure refinement. *J. Chem. Theory Comput.* **2006**, *2*, 1057–1069.
- (19) Friedman, R.; Caflisch, A. On the orientation of the catalytic dyad in aspartic proteases. *Proteins* **2010**, *78*, 1575–1582.
- (20) Cole, J. C.; Murray, C. W.; Nissink, J. W.; Taylor, R. D.; Taylor, R. Comparing protein–ligand docking programs is difficult. *Proteins* **2005**, *60*, 325–332.
- (21) Kitchen, D. B.; Decornez, H.; Furr, J. R.; Bajorath, J. Docking and scoring in virtual screening for drug discovery: Methods and applications. *Nat. Rev. Drug Discov.* **2004**, *3*, 935–949.
- (22) Truchon, J. F.; Bayly, C. I. Evaluating virtual screening methods: Good and bad metrics for the "early recognition" problem. *J. Chem. Inf. Model.* **2007**, *47*, 488–508.
- (23) Bottegoni, G.; Rocchia, W.; Rueda, M.; Abagyan, R.; Cavalli, A. Systematic exploitation of multiple receptor conformations for virtual ligand screening. *PLoS ONE* **2011**, *6*, e18845.
- (24) Totrov, M. Atomic property fields: Generalized 3D pharmacophore potential for automated ligand superposition, pharmacophore elucidation and 3D QSAR. *Chem. Biol. Drug. Des.* **2008**, *71*, 15–27.
- (25) Rueda, M.; Bottegoni, G.; Abagyan, R. Recipes for the selection of experimental protein conformations for virtual screening. *J. Chem. Inf. Model.* **2010**, *50*, 186–193.